J Mater Sci (2010) 45:6018–6024
DOI 10.1007/s10853-010-4685-z

Comparison of magnetic-nanometer titanium dioxide/ferriferous oxide (TiO_2/Fe_3O_4) composite photocatalyst prepared by acid–sol and homogeneous precipitation methods

Jinyuan Chen · Yongxing Qian · Xiuzhen Wei

Received: 2 February 2010 / Accepted: 31 May 2010 / Published online: 15 June 2010
© Springer Science+Business Media, LLC 2010

Abstract Novel magnetic-nanometer titanium dioxide/ferriferous oxide (TiO_2/Fe_3O_4) composite photocatalyst was prepared using acid–sol and homogenous precipitation methods. The photocatalyst particle was made of a Fe_3O_4 core covered with nanocrystal anatase TiO_2, without a high-temperature heat-treatment step. The catalyst has been characterized by X-ray diffraction, transmission electron microscopy, differential thermal analysis measurements, and ultraviolet spectrum. The results suggested that titania was mainly presented as anatase and Fe_3O_4 did not appear on the surface of the composite particles when the molar ratio of TiO_2/Fe_3O_4 increased to 20:1 in the acid–sol method, but 5:1 in the homogeneous precipitin method. The size of the crystal was ranged from 2.4 to 3.6 nm prepared by both methods. In the catalytic test, the composite particles, which were prepared by acid–sol, had higher catalytic activity than that prepared by homogenous precipitation method due to the size difference of the composite particles.

Introduction

TiO_2 is an excellent photocatalyst for its high catalytic efficiency, low toxicity, and good corrosion resistance. It can degrade and mineralize most kinds of organic pollutants, such as dyes, detergents, pesticides, and herbicides [1–6]. However, the practical applications were prohibited due to its two disadvantages. First, low photo-quantum efficiency resulted from the high recombination of photo-generated electrons and holes; second, the electron–hole pairs can only be excited under the UV light. The fact implied that only 3–5% of the solar spectrum can be used. This phenomenon is ascribed to the large band gap (Ebg, anatase $\approx$ 3.2 eV, Ebg, rutile $\approx$ 3.0 eV) of TiO_2 [7]. In order to solve these problems, many methods were developed and doping methods provides a more promising alternative than other methods [8–10].

As for doping elements, transition metals have been extensively used to improve the photocatalytic performance of TiO_2 catalysts [11–14]. At the same time, recycling of TiO_2 is a difficult problem for most of researchers. Since a liquid–solid separation is needed for TiO_2 powders, immobilized photo catalysts are an attractive option for its easy separation from the treated water. However, the degradation efficiency is lower because its less surface area is contacted with pollutants. Watson and coworkers [15–17] prepared $TiO_2/Fe_3O_4/SiO_2$, TiO_2–Fe_3O_4, and FexOy–TiO_2 magnetic composite materials by liquid deposition process, plasma sputtering process, and ultrasonic synthesis process. The effect of high-temperature treatment on phase-conversion phenomenon and photocatalytic activity of TiO_2 were studied. A kind of loaded photocatalyst of TiO_2/Fe_2O_3 (TF), which was prepared by Gao et al. [18], could photo-degrade organic pollutants effectively in the dispersion system and could be recycled easily by a magnetic field. The sample sintered at 500 °C showed the highest activity for the degradation of aqueous solution of acridine dye. Much effort [19–24] was focused on the synthesis of TiO_2/Fe_3O_4, which not only had a great photocatalytic properties, but also could enlarge the range of excitation spectrum and be easily separated by magnetic field for recycling. To the best of our knowledge, however, most of the catalysts had been sintered at high temperature before they could possess high-catalytic activity and no mild methods were applied for obtaining those materials.

J. Chen (✉) · Y. Qian · X. Wei
College of Biological and Environmental Engineering,
Zhejiang University of Technology, Hangzhou 310014, China
e-mail: cjy1128@zjut.edu.cn

In this study, a magnetic nano-material (TiO_2/Fe_3O_4 composite) was synthesized by acid–sol and homogenous precipitation methods, which do not need high-temperature treatment (reaction temperature < 110 °C). As titanium dioxide and ferriferous oxide are transition metal oxides, their physical properties are similar and can coexist. The morphological structure and photocatalytic activities of TiO_2/Fe_3O_4 prepared with two methods were characterized and compared. The morphological structure was characterized with X-ray diffraction (XRD), transmission electron microscopy (TEM), and differential thermal analysis (TG-DTA).The photocatalytic activities of TiO_2/Fe_3O_4 photocatalyst were tested using the dye of active brilliant red X-3B. The analysis of the composite was summarized in our previous article [25], and further analysis and comparison of different particles were presented in this article.

Experimental

Materials

Polyethylene glycol (PEG)-4000 (Shanghai Pudong high-chemical plant in Southern) was used as dispersant; $FeCl_2 \cdot 4H_2O$ (Shanghai chemical plant south field) was used as the source of iron ions. Hydrogen peroxide 30% (Lin'an chemical plant in Zhejiang) was used for getting magnetic fluid; butyl titanate (chemical pure) and dehydrated alcohol (Hangzhou Long March Chemical plant) were used for the synthesis of the titania nanoparticles by acid–sol method. Urea and titanium sulfuric acid were used for the synthesis of the titania nanoparticles by homogenous precipitation method; 14.44 M nitric acid was used as inhibitor to inhibit hydrolysis of butyl titanate. Sodium hydroxide was used to adjust the pH of the solution. All chemicals were of analytical grade. Deionized water (laboratory made) was taken as aqueous media in all experiments.

Synthesis of the photocatalysts

Synthesis of the magnetic fluid

35.5 g PEG and 15 mL H_2O were added to a three-necked flask under ultrasonic vibration. After refluxing for 10 min, the solution reacted by adding 40 mL H_2O drop wise and 1% $FeCl_2$ under nitrogen atmosphere with vigorous stirring. When the solution became uniform, 12 mL 0.06% H_2O_2 was added into the flask. The pH was adjusted to 11–13 with NaOH (3 mol L^{-1}). The reaction was performed at 55°C for 3 h to get the black uniform magnetic fluid. The magnetic fluid was precipitated and separated in magnetic field. The fluid dispersion was washed once every 4 h with deionized water until the magnetic fluid was significantly neutral. Finally, the magnetic fluid was quantitative to 25 mL (solid content: 0.039 g L^{-1}) for further using.

Acid–sol method

TiO_2/Fe_3O_4 composite photocatalysts were prepared by acid–sol method as the following step: 8.5 mL butyl titanate and 10 mL ethanol was mixed to form transparent yellow solution. Then, 20 mL 1 mol L^{-1} HNO_3 was added drop wise with vigorous stirring. After continuous stirring for 1.5 h and adjusting the pH to 1.5 with NaOH (1 mol L^{-1}), a transparent solution (B) was obtained. And then the transparent solution (B) was added to the magnetic fluid (Fe_3O_4), the reaction was performed at pH 6–7 and 100 °C with stirring fiercely for 3 h. The composite photocatalyst was obtained after separating in magnetic field, washing with deionized water, and drying at room temperature for 24 h.

Homogenous precipitation method

In the homogenous precipitation method, titanium dioxide/ferriferous oxide composite was prepared with following procedure: In brief, first the pH of magnetic fluid (Fe_3O_4) was adjusted to 3–4 by 1 mol L^{-1} sulfuric acid solution before 0.1 mol L^{-1} aqueous Ti $(SO_4)_2$ solution was added. Next, 1.2 mol L^{-1} urea was gradually added to the solution under the condition of pH 2–3, temperature 80–100 °C, and vigorous stirring. After neutralization and hydrolysis, the precursor of nano-TiO_2 could gradually packaged on the surface of magnetic Fe_3O_4 nuclear. The process of peptizing and aging with heat treatment was carried out with vigorous stirring for 3 h. The composite photocatalyst was obtained after separating in magnetic field, washing with deionized water, and drying at room temperature for 24 h.

Characterization of photocatalysts

The structure and morphology of TiO_2/Fe_3O_4 composite photocatalyst were characterized by transmission electron microscopy (TEM) JEM-2010 (HR) (Japan); X-ray diffractometer (XRD) Rigaku (D/MAX2550PC) (Japan); surface area meter ASAP 2010 (Micromeritics Instrument Corporation) (N_2 atmosphere determination), and TG-DTA SDT Q600 (TA Instruments) (argon in the atmosphere, warming rate of 10 °C min^{-1}).

Measurements of photocatalytic activities

The photocatalytic activity of each magnetic material was evaluated by the decoloration rate of reactive brilliant red

X-3B dye. Reactive brilliant red X-3B is a common contaminant in industrial wastewater and it has good resistance to light decoloration. 0.1 g magnetic material was added to a beaker containing 50 mL 50 mg L^{-1} reactive brilliant red X-3B solution. And then the mixture was stirred at 30 °C for 30 min to reach the adsorption–desorption equilibrium. A GGZ-300W medium pressure mercury lamp ($\lambda = 365$ nm, Shanghai Dengpao Chang Ya Ming, photodegradation test for distance 20 cm) was used as a UV light source. The analytical samples were separated by centrifugal machine after reacting under UV light for 1 h. The concentration of the filtrate was characterized with U-3400 ultraviolet spectrophotometer at wavelength 540 nm, the maximum absorbance wavelength of dye.

The decoloration rate was calculated using following formula:

$$\text{Decoloration rate} = (1 - A/A_0) \times 100\,\%,$$

where A_0 and A were the absorbance before and after irradiation under UV light, respectively.

Results and discussion

XRD analysis of TiO_2/Fe_3O_4 catalyst prepared at different reaction temperatures

The temperature not only determines the speed of reaction, but also affects the crystal type, yield rate, and stability of the synthesized product in some ways [26]. Figure 1 showed XRD patterns of the composite photocatalyst (TiO_2:Fe_3O_4 = 30:1) prepared at different temperatures by acid–sol method. It could be seen from Fig. 1 that the content of TiO_2 brookite phase (Δ) decreased with the increasing of temperature. The brookite phase would convert to anatase phase (□), which had higher photo-catalytic activity [27, 28] if the temperature increased from 50 to 110 °C. The diffraction peak of Fe_3O_4 could not be found from XRD. The crystallite size of the samples was calculated using the Scherrer's equation: $D = 0.89\lambda/\beta\cos\theta$ [11], where β is the width of the peak at half maximum. The crystallite size of TiO_2/Fe_3O_4 prepared by acid–sol method at different temperatures was 2.2, 2.5, 2.6, 2.8, 3.0, 3.3, 3.8 nm, respectively. It could be seen that the crystallite size enlarged with temperature increasing. The same tendency was observed in Fig. 2. However, it should be noted that the crystallite size of TiO_2/Fe_3O_4 prepared by the acid–sol method was slightly smaller than that of prepared by the homogenous precipitation method. The crystallite size prepared by the latter method was 2.9, 3.3, 3.7, 4.2, 4.6, 4.9 nm, respectively, at different temperatures. The decoloration efficiency of photocatalyst presented as a downward trend due to quantum effect reduced with the

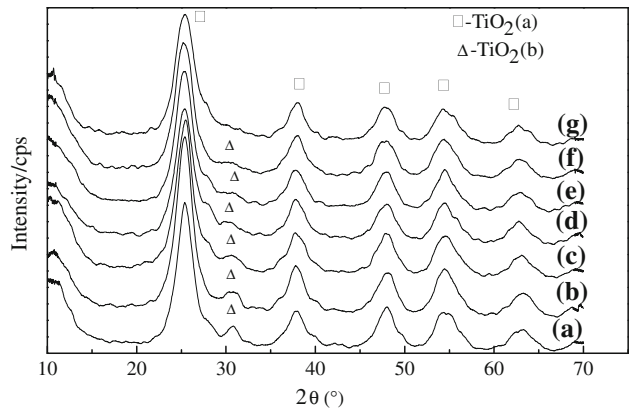

Fig. 1 XRD patterns of the composite material prepared at different temperatures of *a* 50 °C, *b* 60 °C, *c* 70 °C, *d* 80 °C, *e* 90 °C, *f* 100 °C, *g* 110 °C by acid–sol method

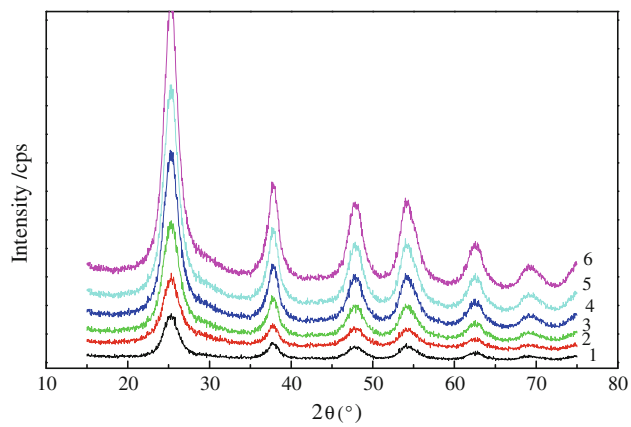

Fig. 2 XRD patterns of the composite material prepared at different reaction temperatures of *1* 70 °C, *2* 80 °C, *3* 90 °C, *4* 100 °C, *5* 110 °C, *6* 120 °C by homogeneous precipitation method

crystallite size increase [29]. Moreover, the hydrolysis of Fe_3O_4 and magnetic fluid was restrained with the temperature increasing, which was harmful to the recovery of catalyst. In order to enhance the hydrolysis, the preparation temperature was strictly controlled at 100 °C.

XRD analysis of TiO_2/Fe_3O_4 catalyst prepared with different ratios

Figures 3 and 4 showed a series of XRD patterns of the photocatalyst. The photocatalyst was prepared by the acid–sol and homogenous precipitation methods with different TiO_2/Fe_3O_4 ratios. In the acid–sol method, there was an obvious peak of Fe_3O_4 when the molar ratio of TiO_2/Fe_3O_4 was smaller than 20:1. When the ratio was increased to 60:1, however, the Fe_3O_4 peak totally disappeared. At the same time, in the homogeneous precipitation method, the peak of Fe_3O_4 did not appear even the ratio of TiO_2/Fe_3O_4

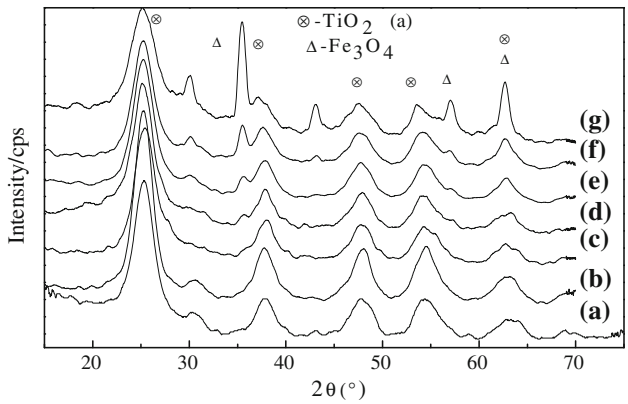

Fig. 3 XRD patterns of TiO_2:Fe_3O_4 catalyst prepared with different ratios of *a* 60:1, *b* 40:1, *c* 30:1, *d* 20:1, *e* 10:1, *f* 4:1, *g* 2:1 by acid–sol method

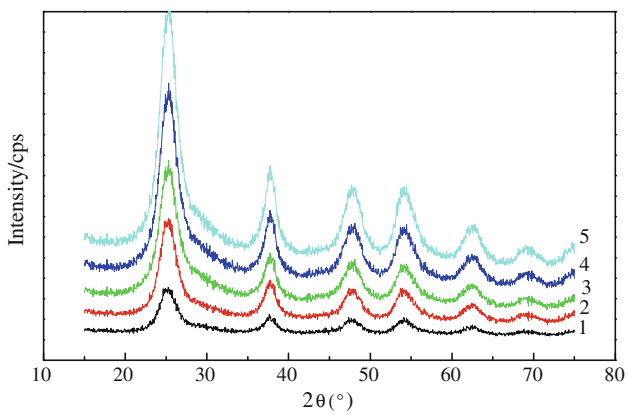

Fig. 4 XRD patterns of TiO_2/Fe_3O_4 catalyst prepared with different ratios of *1* 5:1, *2* 10:1, *3* 20:1, *4* 30:1, *5* 40:1 by homogeneous precipitation method

was 5:1. This phenomenon demonstrated that the small crystal of anatase phase coated tightly on the surface of the Fe_3O_4 core, forming a TiO_2 shell. As both titanium dioxide and ferriferous oxide are transition metal oxide, their physical properties are similar and they can coexist. This indicated that TiO_2 could be released slower to pack on the Fe_3O_4 surface in homogeneous precipitation process than that in acid–sol process.

Further analysis of XRD spectrum showed that the crystal size of TiO_2 particle on the photocatalyst was between 2.4 and 3.6 nm. Most all of TiO_2 covered on the Fe_3O_4 surface was nanometer-crystal with quantum efficiency [30].

TEM image of TiO_2/Fe_3O_4 composite photocatalyst prepared with molar ratio of 30:1

Figure 5 was the TEM image of the Fe_3O_4 core (Fig. 5a) and the composite photocatalyst prepared with TiO_2/Fe_3O_4 ratio of 30:1 by acid–sol (Fig. 5b), and homogenous precipitation method (Fig. 5c), respectively. The Fe_3O_4 particle was mainly presented as cubic form with a size of 8–15 nm. When it was covered up by TiO_2, the particle became spheroid, and the size of composite particles increased to 35–50 nm for the particle prepared by acid–sol method and 60–80 nm for that prepared by homogeneous precipitation method.

In the process of the preparation of composite materials with acid–sol method, nano Fe_3O_4 act as a carrier, which not only had very specific surface area, but also had a large number of oxygen atoms. The oxygen atoms were produced due to broken bonds existing around its surface. A very strong surface bond could be formed between the new born titanium oxide and carrier surface, which could decline the total free energy of the system. The reaction was a very common spontaneous one in the thermodynamic process. Oxides and salts are usually able to spread into single layer on the high-specific carrier surface spontaneously. When the content of TiO_2 was lower than the threshold value, it existed as dispersion form in monolayer or sub-monolayer. It appeared as crystal phase when the content reached the threshold value, TiO_2 content in composite materials was much higher than that of Fe_3O_4, and presented as nano-size particles. It was presumed that TiO_2 could spontaneously disperse on the surface of Fe_3O_4 nuclear in single layer to form a uniform dispersion of TiO_2/Fe_3O_4 composite.

The size of TiO_2/Fe_3O_4 particle prepared by homogeneous precipitation method was larger than that of prepared by acid–sol method. The phenomenon was attributed to the following two reasons. First, the reaction condition of acid–sol method can be controlled easily. Second, in the homogeneous precipitation process, TiO_2 precipitation happens when $CO(NH_4)_2$ and Ti $(SO_4)_2$ are added to the original alkaline solution. However, it is very difficult to control the hydrolysis condition accurately.

TG-DTA curves of TiO_2/Fe_3O_4 nanocomposite material

Figure 6 was the TG-DTA curve of PEG-4000 (Fig. 6a), TiO_2/Fe_3O_4 composite particles prepared by acid–sol (Fig. 6b), and homogeneous precipitation method (Fig. 6c). In the process of TiO_2/Fe_3O_4 materials preparation, PEG-4000 acted as a dispersant, which could prevent agglomerating of TiO_2-coated-Fe_3O_4 nanoparticles. The PEG-4000 on the surface of the composite could be removed completely by repeated washing (this can be judged in TEM figure). TG-DTA curve of PEG-4000 indicated that the endothermic peak of PEG was emerged obviously only at about 331 °C with 99.20% of weight loss. TG-DTA curve of the composite synthesized by acid–sol method indicated

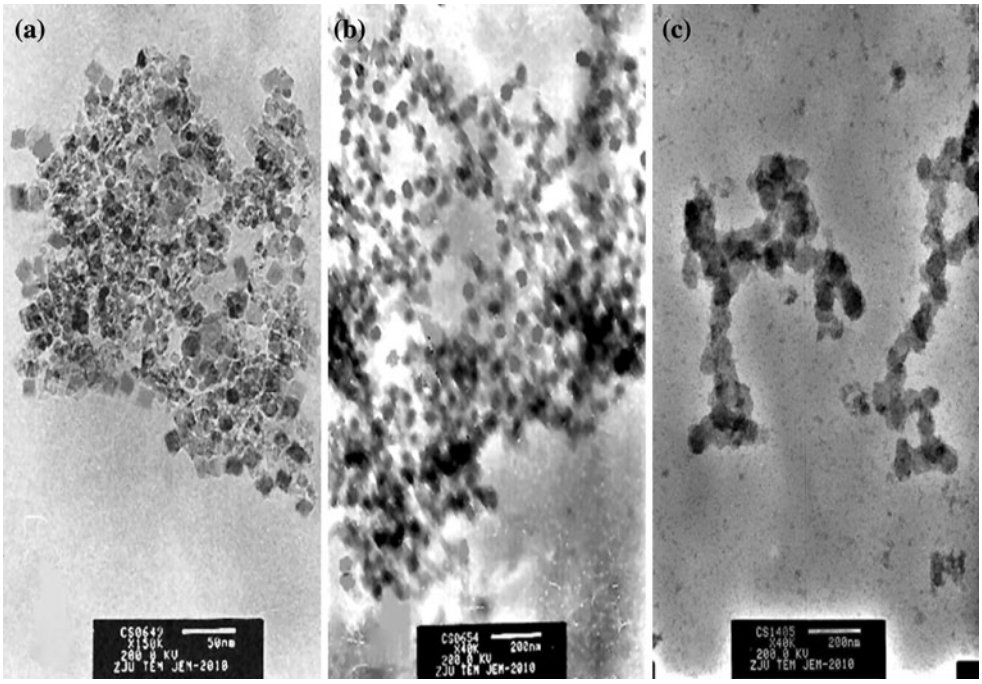

Fig. 5 TEM images of Fe_3O_4 (**a**), the composite material of TiO_2/Fe_3O_4 synthesized by acid–sol method (**b**), and homogeneous precipitation method (**c**)

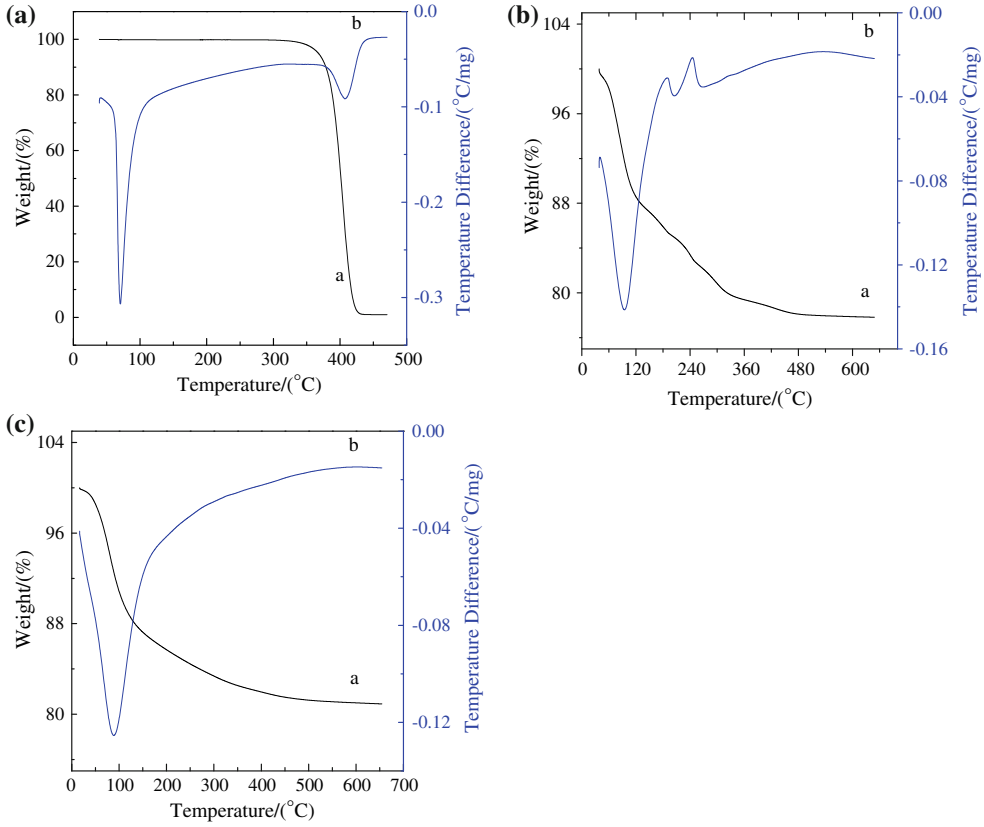

Fig. 6 The TG-DTA curves of PEG-4000 (**a**), TiO_2:Fe_3O_4 nano-composite material synthesized by acid–sol method (**b**), and by homogeneous precipitation method (**c**)

that an endothermic peak was appeared around at 100 °C. At that temperature, 12.57% of the weight loss was appeared due to desorption and volatilization of adsorbed water on the surface of material. And three obvious exothermic peaks were presented with weight loss of 2.305, 2.749, and 3.086% at about 188, 245, and 300 °C,

respectively [31]. However, the TG-DTA curve of the composite synthesized by homogeneous precipitation method indicated that the emergence of endothermic peak with 14.14% of the weight loss was at about 100 °C.

As the control TG-DTA curve of PEG-4000, it was believed that the heating release occurred due to the decomposition of PEG, which was combined in the inner part of composite materials for the existence of TiO_2. When PEG was added to the solution, bare oxygen exposed on the surface of Fe_3O_4 and TiO_2 caused PEG to wind on the surface of magnetic colloidal particles through hydrogen bonds or physical adsorption. At the same time, PEG could form loosen chelated material with Ti^{4+}, steric effect of Ti^{4+} could inhibit aggregation of ions effectively, which reduced the size of the particles and improved the dispersion and uniformity of the $[Ti(HO)_x(H_2O)_{n-x}]^{(4-x)+}$colloidal. As a non-ionic molecule, PEG was not sensitive to the solution containing soluble salts and ionized material, and could form a linear independent space among particles. Thus, the particles could preserve regular space structures, and formed the uniform through-pore structure in the products finally with washing and high-temperature roasting. Moreover, due to PEG also had strong surface activity; it could not only reduce the surface tension of the solution, but also weakened the surface tension and the Vander Waals force between adsorbed water and particles [32]. These can protect the generated particles not to aggregate and finally form dispersed nanoparticles.

The TG-DTA of the composite particles prepared by acid–sol and homogenous precipitation methods was compared. It showed obviously that the materials obtained from acid–sol method had better dispersity, smaller particle size, more bare oxygen exposed on the surface of the materials, and more PEG was combined than that obtained from homogenous precipitation method. All these factors were at key positions to form the unstable structure and more reactive PEG, which induced PEG decomposition at lower temperatures. Thus, the weight loss of TiO_2 prepared by acid–sol method was more than that of prepared by homogeneous precipitation method.

Photocatalytic activity of TiO_2/Fe_3O_4 catalyst

Figure 7 was the degradation curve of TiO_2/Fe_3O_4 prepared by different methods. It was clear that the content of TiO_2 on the surface of the catalyst increased with the increasing of TiO_2/Fe_3O_4 ratio, which induced the photocatalytic degradation activity increased after exposing under UV light for 1 h for TiO_2/Fe_3O_4 prepared with different methods. When the molar ratio of TiO_2:Fe_3O_4 was ranged from 20:1 to 30:1, the catalyst decoloration rate for reactive brilliant red X-3B could reach 100 and 97.12% for the TiO_2/Fe_3O_4 prepared with acid–sol method and homogeneous precipitation method, respectively. For pure nano-TiO_2, however, the decoloration rate was only 95.3%. This indicated that the composite TiO_2/Fe_3O_4 has better photocatalytic activity than pure nano-TiO_2 [33]. The decoloration rate was decreased until the ratio exceeds 40:1.

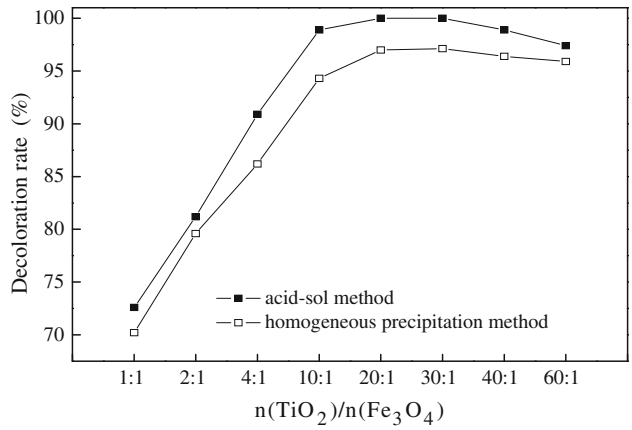

Fig. 7 Curves of photocatalytic decoloration rate of TiO_2/Fe_3O_4 catalyst with different ratios by acid–sol and homogeneous precipitation methods

The reasons for the catalyst efficiency improving can be explained as follows. On the one hand, few free Fe^{3+} ions exist in magnetic Fe_3O_4 and the composite materials were synthesized fiercely and continuously. The radius of Ti^{4+} six-coordinated complexes (74.5 nm) are similar with that of Fe^{3+} six-coordinated complexes (69 nm) and Ti^{4+} is a multivalent ion with under-filled *d* orbit. Thus, the lattice of Ti^{4+} could be occupied easily by Fe^{3+}, during TiO_2 nanocrystals formation process, which lead to the generation of the defect [34]. Fe^{3+} can also serve as an electron capture agent because the energy level of Fe^{3+}/Fe^{2+} is close to the energy level of TiO_2 conduction band [35]. The replacement of Ti^{4+} by Fe^{3+} improves the capability of capturing electric load flow, prolongs the life of electron–hole pairs, and increases the photocatalytic activity. On the other hand, the electron captured by Fe^{3+} can easily transfer to the surface of Ti^{4+}. Generally speaking, electrical current load-transfer reaction is a slow process (nearly to 1 s), and interfacial charge transfer occurs in milliseconds. As for the nanocatalysts, due to lack of the bond belt bending, electron–hole pairs can easily coexist or very close to the interface, and cause electron to transmit easily, which can also improve the photocatalytic activity [36].

The degradation efficiency of catalyst (decoloration rate) was decreased with the increasing of TiO_2/Fe_3O_4 ratio. This was attributed to the following two reasons. First, under the condition of low proportion of Fe_3O_4 in the composite TiO_2/Fe_3O_4, few relative infiltrate Fe^{3+} may cause few defect location on the surface of TiO_2, which

cannot inhibit the recombination of electron–hole pairs [37]. Second, too much TiO_2 was coated on the surface of Fe_3O_4, which resulted in an excessive recombination of electron–hole pairs, impacted the formation of hydroxyl radicals, and reduced the utilization of light.

Conclusions

TiO_2/Fe_3O_4 photocatalyst was prepared by acid–sol and homogenous precipitation methods. Temperature and the content of TiO_2 in the photocatalyst were the mainly factors, which affect the synthesis of the TiO_2/Fe_3O_4 photocatalyst. The results showed that the nanocrystal of TiO_2 was the anatase with a magnetic Fe_3O_4 core. The TiO_2 crystal size was 2.4–3.6 nm, while the size of composite particles prepared by acid–sol and homogenous precipitation methods were ranged from 35 to 50 and 60 to 80 nm, respectively. It was found that the TiO_2/Fe_3O_4 photocatalyst prepared by acid–sol method exhibited better morphological structure and photocatalytic activity than that prepared by homogenous precipitation method. TiO_2/Fe_3O_4 prepared by the two methods showed better photocatalytic activity than that of pure nano-TiO_2. And TiO_2/Fe_3O_4 composite catalyst could be obtained without heat treatment at high temperature.

Acknowledgements The authors would like to acknowledge financial support for this work provided by the National Science Foundation of China (No. 20877070) and the National Science Foundation of Zhejiang Province (No. Y5080233).

References

1. Tokumura M, Znad HT, Kawase Y (2008) Water Res 42:4665
2. Kurinobu S, Tsurusaki K, Natui Y et al (2007) J Magn Magn Mater 310:1025
3. Go′rska P, Zaleska A, Kowalska E et al (2008) Appl Catal B Environ 84:440
4. Fujishima A, Zhang XT, Tryk DA (2007) Int J Hydrogen Energy 32:2664
5. Sohrabi MR, Ghavami M (2008) J Hazard Mater 153:1235
6. Makgae ME, Klink MJ, Crouch AM (2008) Appl Catal B Environ 84:659
7. Tong TZ, Zhang JL, Tian BZ (2008) J Hazard Mater 155:572
8. Yu QH, Zhou CG, Wang X (2008) J Mol Catal A Chem 283:23
9. Wang C, Yang GM, Li J et al (2009) Dyes Pigments 80:321
10. Delgado FG, Go′mez KV (2008) Microelectron J 39:1333
11. Quan XJ, Zhao QH, Tan HQ et al (2008) Mater Chem Phys 114:90
12. Son JH, Kim SW, Bae DS et al (2008) Mater Sci Eng A 498:2
13. Sharma SD, Saini KK, Kant C et al (2008) Appl Catal B Environ 84:233
14. Calle M, Sa′nchez LC, Arboleda JD et al (2008) Microelectron J 39:1322
15. Watson S, Beydoun D, Amal R (2002) J Photochem Photobiol A Chem 148:303
16. Ye FX, Ohmori A (2002) Surf Coat Technol 160:62
17. Huang WP, Tang XH (2002) Mater Res Bull 37:1721
18. Gao Y, Chen BH, Li HL et al (2003) Chem Phys 80:348
19. Beydoun D, Amal R (2002) Mater Sci Eng B 94:71
20. Gad-Allah TA, Fujimura K, Kato S et al (2008) J Hazard Mater 154:572
21. Wang J, Yang PP, Fan MQ et al (2007) Mater Lett 61:2235
22. Gad-Allah TA, Kato S, Satokawa S et al (2007) Solid State Sci 9:737
23. Ling QC, Sun JZ, Zhou QY et al (2008) Photobiol A Chem 200:141
24. Tawkaew S, Supothina S (2008) Mater Chem Phys 108:147
25. Chen JY, Zhang GL (2006) In: Abstracts of papers of the American Chemical Society, p 26
26. Zan L, Zhong JC, Luo QR (1999) J Inorganic Mater 14:264
27. Grieken R, Aguado J, Lōpez-Muoz MJ et al (2002) Photochem Photobiol A Chem 148:315
28. Moazzem HM, Raupp GB (1999) Chem Eng Sci 54:3027
29. Harada H, Ueda T (1984) Chem Phys Lett 106:229
30. Mazzarino I, Piccinini P (1999) Chem Eng Sci 54:3107
31. Sun JL, Jiao LF, Wei X (2010) J Solid State Electrochem 14:615
32. Rouquerol F, Rouquerol J, Sing K (1999) Adsorption by powders and porous solids: principles, methodology and applications. Harcourt Brace & Company, Academic Press, London, p 205
33. Misook K, Choung SK, Jong YP (2003) Catal Today 87:87
34. Jin HF, Li WG, Xiang JM et al (2001) Chin J Appl Chem 18:636
35. Mo SD, Lin LB, Lin DL (1994) J Phys Chem 55:1309
36. Thompson TL, Yates JTJ (2006) Chem Rev 106:4428
37. Su B, Zhang Z, Zheng J (2002) Acta Chim Sin 60:1936